Solar Energy 195 (2020) 185–193

Contents lists available at ScienceDirect

Solar Energy

journal homepage: www.elsevier.com/locate/solener

Evaluation of thermal performance for a smart switchable adaptive polymer dispersed liquid crystal (PDLC) glazing

Abdulmohsin Hemaida, Aritra Ghosh, Senthilarasu Sundaram, Tapas K. Mallick*

Environment and Sustainability Institute (ESI), University of Exeter, Penryn Campus, TR10 9FE, United Kingdom

ARTICLE INFO

Keywords:
Glazing
PDLC glazing
Smart window
Optical properties
Solar heat gain coefficient (SHGC)
Thermal performance (*U*-value)

ABSTRACT

A new class of smart window technologies are gaining interest as they have the functionality to control dynamic solar radiation, shading, ventilation and energy production. They are capable of improving buildings' energy performance by adapting to different climate conditions and bring thermal and visual comfort for occupants. Polymer-dispersed liquid crystal (PDLC) is a smart switchable window that changes its optical transmissions from translucent to transparent when an alternating electric current stimulus is introduced. The present paper discusses the results of an indoor investigation for the optical and thermal performance of a PDLC glazing system. The spectral transmittance of the investigated PDLC was evaluated for both the translucent and transparent states using UV–vis–NIR (1050) spectrophotometer. In addition, the thermal investigation was carried out in an indoor condition utilising a test cell equipped with a small scale of PDLC glazing, which was exposed to (1000, 800, 600, 400 W/m^2) solar radiation for 180 min. The optical evaluation showed that the investigated PDLC glazing offered low transmission for UV (8%) and NIR (44%) in the translucent state, respectively. The result of SHGC was 0.68 and 0.63 for the transparent and translucent states, respectively, which indicates that the investigated sample could be more effective in reducing heat loads in a cold dominated climate. The *U*-value for the PDLC glazing was 2.79 W/m^2 for the transparent and 2.44 W/m^2 translucent.

1. Introduction

In the European Union (EU), the building sector utilises 40% of total energy consumption, which is responsible for 36% of CO_2 emissions (Salem et al., 2019). The residential building sector is consuming 25% energy, leading to 16% greenhouse gas emissions (European Commission, 2019). Building activities such as cooling, heating, and lighting contribute to a significant concern related to environmental issues and energy demand (Dussault et al., 2012). In this respect, it is essential to take decisive measures to reduce global energy demand and greenhouse gas emission. Conventional building components particularly window exhibit poor thermal insulation that significantly affects the energy performance of a building and wellbeing of occupants.

In recent years, considerable interest has been given towards saving energy, which is usually associated with windows' performance due to their high overall heat coefficient (*U*-value) compared to other building components (Cuce, 2014). Windows in buildings offer a vision of the outside environment and enable air ventilation, sunlight, and passive solar gain. However, windows are responsible for approximately 60% of the total energy consumed in a building due to the high overall heat loss and heat gain (Rezaei et al., 2017). *U*-value and solar heat gain coefficient (SHGC) are the major two factors that determine windows' energy performance. In cold climates, high SHGC is desirable in reducing heating loads, whereas low SHGC is more beneficial in hot climates in order to lower cooling loads (Kuhn, 2014). In this regard, it is essential that windows have appropriate SHGC and *U*-values to bring thermal comfort to occupants, as well as minimise energy demands. In addition, solar radiation also could affect the wellbeing of occupants and degradation of materials inside a building. This can be measured by solar material protection factor (SMPF) and solar skin protection factor (SSMF) (Jelle et al., 2007).

Dynamic tintable windows are a new class of windows and can change optical and thermal properties according to occupants' needs in response to an electric stimulus or changing environmental conditions (Casini, 2018). Additionally, dynamic switchable windows and their building applications would have a considerable impact on reducing energy consumption and artificial lighting (Granqvist et al., 2017). A large number of research studies are available in the literature for electrically switchable windows, such as: electrochromic (EC) windows (Baloukas et al., 2017; Tavares et al., 2016); suspended particles device (SPD) (Al Dakheel and Aoul, 2017); and liquid crystal (LC) (Jung et al., 2017; Oh et al., 2019; Torres et al., 2014).

* Corresponding author.
E-mail address: T.K.Mallick@exeter.ac.uk (T.K. Mallick).

https://doi.org/10.1016/j.solener.2019.11.024
Received 4 August 2019; Received in revised form 31 October 2019; Accepted 6 November 2019
Available online 26 November 2019

Nomenclature

A_{PDLC}	Aperture area of PDLC glazing (m^2)
A_{wall}	Interior wall surface area (m^2)
C_{air}	Heat capacity of air (kJ/kg K)
h_o	Heat transfer coefficient from test cell outer surface (W/m^2 K)
h_i	Heat transfer coefficient from test cell inside surface (W/m^2 K)
I	Incident radiation (W/m^2)
K_{pl}	Thermal conductivity of polystyrene (W/mK)
L_{pl}	Thickness of polystyrene (m)
τ_{dir}	Direct transmittance
τ_{diff}	Diffuse transmittance
S_{uv} (λ)	Relative spectral distribution of ultraviolet solar radiation
D_{65}	Distribution of illuminant
V(λ)	Spectral efficiency of a standard photopic observer
M_{tc}	Mass of the air inside test cell (kg)
$T_{in,tc}$	Interior temperature of test cell (°C)
$T_{out,tc}$	Ambient temperature (°C)
U_{PDLC}	Overall heat transfer coefficient of glazing (W/m^2 K)
Q_{in}	Incident radiation on glazing (W)
Q_{loss}	Total heat loss through the glazing (W)
Q_{PDLC}	Total heat transfer through the glazing (W)
$Q_{testcell}$	Total heat inside the test cell (W)
α	Absorptance
τ	Transmittance
T (λ)	Spectral transmission of glazing
R (λ)	Reflection of glazing
S(λ)	Spectral distribution of solar radiation

EC windows change their colour reversibly due to the oxidation and reduction reaction when an electrical field is applied (Casini, 2018). They are capable of controlling solar radiation by modulating visible and thermal transmittance (Casini, 2018). Dynamic EC glazing also has the potential to control near-infrared (NIR), which can save up to 5–15 kWh/m^2 year of the heating and cooling loads of commercial and residential buildings (Sbar et al., 2012). Solar heat gain coefficient has been observed in EC windows at 0.49 in the clear state, and 0.09 in the full dark state with light transmission values ranging between 69% and 1%, respectively. An investigation of a dynamic EC window has reported that EC can modulate visible transmission from 62% with 0.47 SHGC to fully dark state with ≤2% and 0.09 SHGC (Sbar et al., 2012). The switching time of EC devices is reasonably slow, for instance, a 1.2 m × 0.8 m glazing requires approximately 12 min to change to the dark state (Tavares et al., 2016), whereas SPDs take a few seconds to change to fully translucent/dark state (Ghosh and Norton, 2018).

In a recent study, the performance of EC double glazing was investigated with respect to solar radiation control and the energy demand for residential buildings for Italian weather (Piccolo et al., 2018). The EC glazing was synthesised of WO_3 as the active layer and NiOH:Li as the ion storage layer and deposited on 12 × 12 cm^2 FTO glass substrates. The investigated glazing switches colour reversibly from clear state to a dark blue with a potential ± 2.5 V and switching time 5–6 min. It was concluded that this EC glazing is effective in reducing heat loads during the summer months. The EC glazing, however, generated secondary heat gain that could raise the temperature of the internal glass, which may result in thermal discomfort for occupants. SPDs comprises of a polymer layer, which has light-absorbing and polarisable particles that are sandwiched between two transparent conductive thin films (Barrios et al., 2013). The optical properties of SPDs are altered by applying the alternating power supply to the active layer, which results in the particles becoming parallel and yield a higher transmittance “on-state”. Meanwhile, the absence of a power supply results randomly oriented particles and produces lower transmittance “off-state” (Barrios et al., 2013). SPDs can offer comfortable daylight with transmissions varying from 5% in the dark state to 55% in the transparent state (Ghosh and Norton, 2017). In addition, SPDs can control the solar heat gain from 0.05 to 0.38 in the translucent and transparent states, respectively (Ghosh et al., 2016a).

Electrically switchable liquid crystal device windows change their transparency when an electrical field is introduced (Huang et al., 2019). Polymer dispersed liquid crystal (PDLC) is potentially suitable glazing for building applications, as it can be operated without polarisers, have high transparency transmission, large viewing angle, fast switching time, absence of surface treatment and the potential of controlling the transmission level (Torres et al., 2014). Generally, PDLC films, within a solid polymer matrix, are composed of lower molecular weight micro-sized droplets of liquid crystal. These are situated between two separate transparent conducting electrodes. In the absence of power, due to the refractive index mismatch between droplets and the polymer matrix, PDLC scatters lights. Moreover, when the power supply is present, LC molecules are oriented to enable light to pass through meaning the refractive index between the polymer matrix and the droplets match. The droplets’ sizes define PDLC scattering, while the radius of the droplets is smaller than the incident wavelength, which enables light to pass through without any form of scattering. Indoor spectral characterisation of a PDLC glazing size of 0.2 × 0.15 m offered visible transmission of 71% for transparent state and 27% for the translucent state, while SHGC varied from 0.53 to 0.39 for the transparent and translucent states, respectively (Ghosh and Mallick, 2018a). A study has proposed a smart system to reduce energy consumption using smart PDLC glass (Hisham, A. and Amawgani, 2019). The proposed system utilised a programmable Arduino light sensor to detect the sun movement and automatically change its shading mode gradually by remote control according to the user desire. The study reported that the system could produce 39% of energy reduction compared to the conventional window systems. PDLC films have shown excellent performance blocking UV, which is recorded as up to 98% and modulating the NIR in the range between 12 and 38%. Moreover, PDLC films have shown excellent durability with 3 million cycles at applied voltage 100 VAC, 60 Hz and with a switching interval of 1 sec (Park and Hong, 2009). In comparison, EC devices can sustain a lifetime of 10^5 cycles with an operating temperature between −30 to 60 °C (Piccolo and Simone, 2015). Thermal performance of an EC glazing was investigated using a PASSYS test cell that showed a *U*-value of 3.8 W/m^2 K and SHGC 0.47 and 0.09 for hot and cold climates, respectively (Sbar et al., 2012). The thermal characterisation of SPD has been investigated using a test cell in Dublin which showed overall heat transfer coefficient for the SPD at 5.9 W/m^2 K, while the SPD double glazing was 2.98 W/m^2 K for both states (Ghosh et al., 2015).

PDLC glazing can change its transmission according to the users’ needs by varying the voltage (Ghosh and Mallick, 2018b). Although PDLC glazing suffers from haze, manufacturers are investigating to produce haze-free PDLC (Hakemi et al., 2018). Generally, PDLC glazing is used for solar energy control, along with aesthetic and privacy applications. The conventional window systems were insufficient in providing energy efficiency for buildings and environmental wellbeing required by regulations (Casini, 2015). In contrast, PDLC glazing systems are electrically switchable windows that are employed in the green building to provide benefits such as energy reduction for heating, cooling, and artificial lighting as well as brings visual comfort for the building inhabitants. The technology of PDLC glazing controls the incoming solar radiation by modulating the glazing transmissions and potentially lead to energy efficiency and improve wellbeing. Furthermore, PDLC can be manufactured as a laminated thin film, which can be an excellent option for retrofit applications (Oh et al., 2019). However,

far too little attention has been paid to understand the thermal performance of PDLC glazing in the existing literature. Therefore, the study aims to investigate particularly the *U*-value and SHGC of a PDLC glazing system conducted under indoor conditions by utilising a small-scale test cell equipped with small area of PDLC glazing and temperature sensors to measure the solar energy entering the test cell through the PDLC glazing. In addition, optical characteristics and protection factors were also evaluated. The results of this work will be beneficial for building engineers to incorporate in the retrofit or design of a new low energy building with PDLC switchable glazing.

2. Methodology

The optical characterisation was performed for the PDLC film using a spectrophotometer to measure the solar transmittance and reflectance at a wavelength (300–2500 nm) for both the translucent and transparent states. In addition, the thermal performance of the PDLC glazing was characterised by solar heat gain (SHGC) and thermal transmission (*U*-value). Both SHGC and *U*-value have similar effects on a building indoor environment.

Calorimetric approach is useful to determine the thermal transmission and solar heat gain. The operation of outdoor calorimeters can be significantly affected by the environmental conditions, while the operation of the indoor calorimeters can be controlled. In outdoor experiments, the specimen facing the environment cannot be controlled that could affect the value of the SHGC (Simmler and Binder, 2008; Tait, 2006). The investigation of the PDLC glazing system was conducted in an indoor environment to eliminate the effects of the outdoor environmental conditions and obtain accurate measurements. The solar heat gain and thermal transmittance of the PDLC system were investigated in an indoor facility considering only the glass.

2.1. Optical properties of PDLC glazing

The solar radiation reaches the earth's surface, including visible light (VIS), ultraviolet (UV), and near-infrared (NIR) is approximately located between (300 nm and 3000 nm). The visible light is located between (380 nm and 780 nm) while the UV and NIR are located below and above the VIS spectrum. When the incident solar radiation falls onto glazing, it will be transmitted, reflected, and absorbed. The optical properties of the glazing, the incident angle, and the wavelength of the radiation determine the amount of solar radiation that is transmitted, reflected, and absorbed. Furthermore, the optical properties influence the transmitted solar radiation to produce distinct incident angle dependencies applied to the different relative intensity of the components of direct, diffuse, and ground reflected solar radiation. The diffuse light can determine the satisfaction of a room illumination whereas; the direct solar radiation influences the solar material protection factor and the skin solar protection factor (Jelle et al., 2007). The high energy of solar radiation like UV can have a negative impact on the glazing lifetime, the interior building materials, and human skin. Thus, such knowledge is important to determine what type of glazing should be used for low energy building.

In order to evaluate the optical characteristics of the PDLC glazing system, a spectrophotometer was employed to measure the solar transmission and reflection. The UV transmittance, visible transmittance and reflectance, solar transmittance and reflectance, and solar absorption, were calculated using the following equations (1–6) (I.S.O 9050, 2003):

$$\text{UV transmittance } \tau_{uv} = \frac{\sum_{\lambda=300}^{380nm} T(\lambda) S_\lambda \Delta\lambda}{\sum_{\lambda=300}^{380nm} S_\lambda(\lambda)\Delta\lambda} \quad (1)$$

$$\text{Visible transmittance } \tau_{vis} = \frac{\sum_{\lambda=380nm}^{780nm} T(\lambda) D_{65}(\lambda) V(\lambda)\Delta\lambda}{\sum_{\lambda=380nm}^{780nm} D_{65}(\lambda) V(\lambda)\Delta\lambda} \quad (2)$$

$$\text{Visible reflectance } R_{vis} = \frac{\sum_{\lambda=380nm}^{780nm} D_{65}(\lambda) R(\lambda) V(\lambda)\Delta\lambda}{\sum_{\lambda=380nm}^{780nm} D_{65}(\lambda) V(\lambda)\Delta\lambda} \quad (3)$$

$$\text{Solar transmittance } \tau_{sol} = \frac{\sum_{\lambda=300nm}^{2500nm} T(\lambda) S(\lambda)\Delta\lambda}{\sum_{\lambda=300nm}^{2500nm} S(\lambda)\Delta\lambda} \quad (4)$$

$$\text{Solar reflectance } R_{sol} = \frac{\sum_{\lambda=300}^{2500nm} R(\lambda) S(\lambda)\Delta\lambda}{\sum_{\lambda=300nm}^{2500nm} S(\lambda)\Delta\lambda} \quad (5)$$

where, S_{uv} (λ) is the relative spectral distribution of ultraviolet solar radiation. D_{65} is the relative distribution of illuminant D65, V(λ), which is the spectral efficiency of a standard photopic observer, S(λ) relative spectral distribution of solar radiation, and Δλ is the wavelength interval. T (λ) and R (λ) are the spectral transmission and reflection of glazing. In addition, solar absorption is calculated using the written Eq. (6):

$$\text{Solar absorption} \alpha_s = 1 - \tau_s - \rho_s \quad (6)$$

The selectivity index is the ratio of light transmissivity with the total transmitted energy from the glazing. The higher the value of the selectivity index, the better the solar control performance for glazing. Haze percentage was determined for the considered glazing using Eq. (8), where T_d and T_{Total} illustrate the diffuse and total transmission.

$$Selectivity = \frac{\tau_v}{g} \quad (7)$$

$$Haze = \frac{T_d}{T_{Total}} 100\% \quad (8)$$

2.2. Evaluation of solar material protection and solar skin protection factor

Some part of the solar radiation such as the ultraviolet and visible spectrum can have a negative impact on human skin and materials inside a building. The impact on materials varies from discolouration to loss of functionality, while human skin may experience pale skin to severe sunburn. The level of damage depends on the time and degree of exposure. The level of impact for human skin might be minimised by clothing and sun lotions, while the light stabiliser application may protect the materials. PDLC glazings can be of interest in this aspect as they have the potential to control the solar radiation. This section aims to evaluate how well the PDLC glazing system protects human skin and materials inside buildings from the solar radiation. In order to measure the protection level, the solar material protection factor (SMPF), and solar skin protection factor (SSPF) was calculated. The values of (SMPF) and (SSPF) range from 0 to 1, where a higher value indicates a high protection level (Jelle, 2013). To show that a larger part of the visible solar spectrum can degrade materials, the SMPF was calculated in the wavelength of today's value between 300 nm and 600 instead of the earlier value 300 nm–500 nm (I.S.O 9050, 2003). The evaluation of (SMPF) and (SSPF) was achieved by a mathematical calculation.

Solar material protection factor

$$\text{SMPF} = 1 - \frac{\sum_{\lambda=300nm}^{600nm} T(\lambda) C_\lambda S_\lambda \Delta_\lambda}{\sum_{\lambda=300nm}^{600nm} C_\lambda S_\lambda \Delta_\lambda} \quad (9)$$

where $C_\lambda = e^{-0.012\lambda}$

Solar skin protection factor

$$\text{SSPF} = 1 - \frac{\sum_{\lambda=300nm}^{400nm} T(\lambda) C_\lambda S_\lambda \Delta_\lambda}{\sum_{\lambda=300nm}^{400nm} E_\lambda S_\lambda \Delta_\lambda} \quad (10)$$

E_λ CIE erythermal effectiveness.

2.3. Solar heat gain coefficient

Solar heat gain coefficient (SHGC) is the fraction of incident solar

radiation that passes through a glazing system to a room in the form of transmitted radiation (Goia and Serra, 2018). The solar gain passively causes the room temperature to rise, which is desirable during the winter season, although not during the summer months. SHGC is a primary factor to evaluate the glazing system and the energy consumption of a building (Kuhn, 2014). SHGC can be influenced by several elements such as the wind conditions, the spectrum of the incident radiation, and the internal and external temperature, however, the wind condition is neglected in this case (Kuhn, 2017). Thus, the SHGC was calculated for the PDLC glass by the following equation.

The solar heat gain coefficient can be calculated by Eq. (11) (I.S.O 9050, 2003; Institution, 1998).

$$g = \tau_s + q_i = \tau_s + \alpha\frac{h_i}{h_i + h_e} \tag{11}$$

where h_i and h_e stand for the internal and external heat transfer coefficient, τ_s represents solar transmittance, and α is the solar absorbance.

2.4. Overall heat transfer coefficient

Thermal transmission through a glazing system is determined by the difference of temperature between external and internal surfaces with consideration of the thermal conduction, convection, and radiation (Chae et al., 2014). Room temperature is usually maintained constant, whereas the external temperature varies based on environmental conditions, such as solar radiation and wind velocity. Overall heat transfer coefficient determines how well a glazing system can insulate heat loss from inside of a room to the outside environment. Therefore, the *U*-value of the PDLC glass was determined using mathematical models.

Overall, the heat transfer coefficient can be calculated by Eq. (17) (Ghosh et al., 2018, 2015). The parameters required to calculate *U*-value are presented in Table 1.

$$Q_{in} = Q_{PDLC} + Q_{testcell} + Q_{loss} \tag{12}$$

where Q_{in} is the incident radiation.

Q_{in} can be calculated using Eq (12).

$$Q_{in} = I\alpha\tau A_{PDLC} \tag{13}$$

Total heat transfer through the glazing is expressed in Eq (10) (Ghosh et al., 2016b).

$$Q_{PDLC} = U_{PDLC}A_{PDLC}\Delta T \tag{14}$$

Total heat transfer inside the test cell is provided by (Ghosh et al., 2016a).

$$Q_{testcell} = m_{testcell}C_{air}\frac{dT}{dt} \tag{15}$$

The total heat losses through the test cell are given by

$$Q_{loss} = (UA)_{testcell}(\Delta T) \tag{16}$$

Overall heat transfer of the PDLC glazing is calculated using Eq (17)

$$U_{PDLC} = \frac{Q_{in} - Q_{testcell} - Q_{loss}}{A_{PDLC}\Delta T} \tag{17}$$

3. Experimental procedure

In an effort to investigate the PDLC glazing system, various materials and equipment were utilised. The following paragraphs provide a description of the PDLC glazing system and all the equipment employed to investigate the PDLC optical properties, solar heat gain, and thermal transmittance.

3.1. The PDLC glazing system

The PDLC film employed in this study was purchased from the HOHO industry. The size of the PDLC film is 0.15 m^2 × 0.142 m^2 and switches from a translucent to transparent state when a potential 20 V AC is applied. It consists of a 20 μm polymer layer sandwiched between two 188 μm ITO layers. The PDLC film was sandwiched between two low iron glasses where each glass was 4 mm thick and then was attached on the top of a test cell. The test cell comprised of 2.5 mm thick polystyrene and dimensions of 0.36 m × 0.186 m × 0.245 m. The system was used to characterise the optical properties, solar heat gain and thermal transmittance of PDLC glazing. Fig. 1 demonstrates the PDLC film in the transparent state (ON) while the particles are aligned and allow light transmission. In the translucent state, particles dispersed in PDLC film are randomly oriented and transmit low light.

3.2. Spectrophotometer measurement

The measurement was undertaken using a Perkin Elmer® Lambda 1050 UV/VIS/NIR spectrophotometer to evaluate the solar transmissions of the PDLC glazing system. The instrument features a double-beam; double-monochromator; ratio recording optical system; and a LabSphere 150 mm. The sphere feature enables an effective collection surface for the detectors, equivalent to the sphere input ports area (1 in./25.4 mm). Specifically, Fig. 2 illustrates the schematic diagram of Perkin Elmer® Lambda 1050 UV/VIS/NIR spectrophotometer.

3.3. Indoor solar simulator

The test cell was placed under a light beam of a AAA type indoor solar simulator, which has a similar spectrum to the solar spectrum between 250 nm and 3000 nm. A Pico data logger was employed to record the temperature with a 5 min interval time. Several thermocouples type T were used to measure the external and internal glass surfaces, inner test cell, and ambient laboratory temperature. Fig. 3 below shows a photograph of the experiment setup.

Table 1
Parameters required to calculate U-value.

Fixed Parameters		Value
	Aperture area of glazing (A_{PDLC})	0.021 m^2
	Interior wall surface (A_{wall})	0.401 m^2
	Internal volume of test cell (v_{air})	0.0164 m^3
	Thickness of Polystyrene (L_{pl})	0.025 m
	Mass of air inside test cell ($M_{tc} = v_{air} \times \rho_{air}$)	0.02 kg
Physical	Density of air (ρ_{air})	1.2250 kg/m^3
	Heat capacity of air (C_{air})	1.006 kJ/kg K
	Thermal conductivity of polystyrene (K_{pl})	0.038 W/mK
	Incident radiation from simulator (I)	1000 (W/m^2)
Variables	Temperature inside the test cell ($T_{in,tc}$)	Measured by thermocouple (T)
	Temperature outside the test cell ($T_{out,tc}$)	Measured by thermocouple (T)

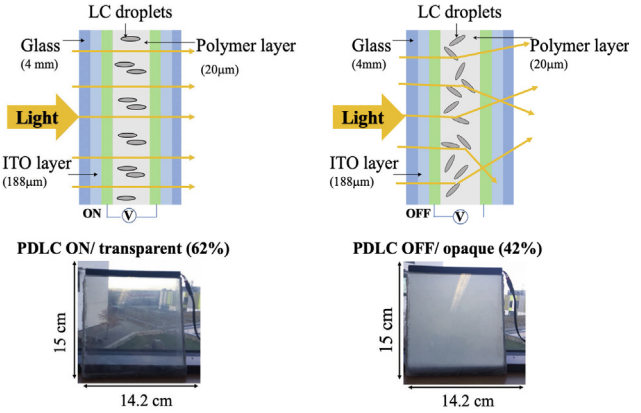

Fig. 1. The PDLC design shows that the particles are aligned when the power supply is ON, and light passes through the glazing. When the power supply is OFF the liquid crystal particles are randomly aligned in the polymer resulting in a translucent state. The thickness of the layers and the glazing size are presented.

4. Results and discussion

Comprehensive review for the results of the solar transmission, solar protection factors, SHGC, and *U*-value are discussed in relation to the solar radiation in the following paragraphs.

4.1. PDLC transmission measurements

Fig. 4 shows the measured total transmission of the PDLC glazing by using a spectrophotometer, with results of 62% for the transparent state and 42% for the translucent state. The PDLC glazing offered UV transmission of 17% in the transparent state and 8% in the translucent state. It controlled the NIR radiation by 44% in the translucent state and 61% in the transparent state. Moreover, PDLC scatters light, starting from the edges or conductive electrode, and increases towards the centre. This process occurs because the refractive index does not match between the droplets and the polymer matrix during the translucent state. Comparatively, when PDLC is in the transparent state, the LC molecules align and enable light to pass through, which indicates that the refractive index between the polymer matrix and droplets are matched. The spectrophotometer measurements demonstrate that the diffused light was collected by the sphere from both states and scattered forward. Besides, the LC particles make the light scatter, resulting in higher transmission during the translucent state.

The same figure reports that the total reflectance of PDLC glazing for both states was very similar, which indicates that there was no backscattering. The reflectance during the translucent state was 18%, and during the transparent state was 17%. It was found that this PDLC glazing reflected 14% of UV radiation in the transparent state and 18% in the translucent state. In the NIR region, the reflection was 15% and 16% for the transparent and translucent states, respectively. Solar

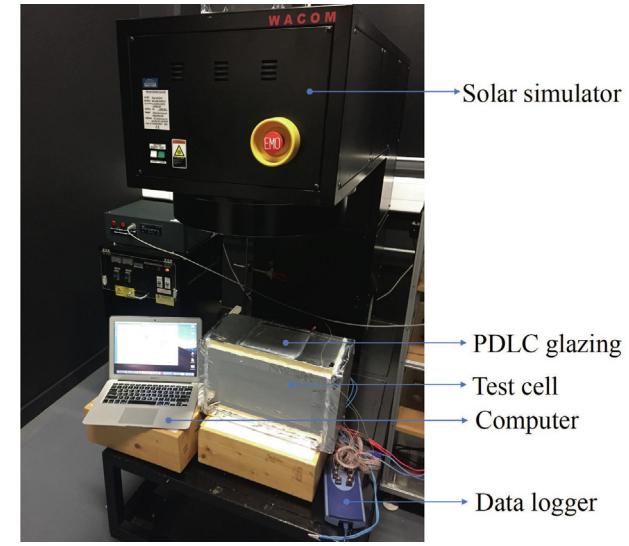

Fig. 3. Photograph of the experimental setup.

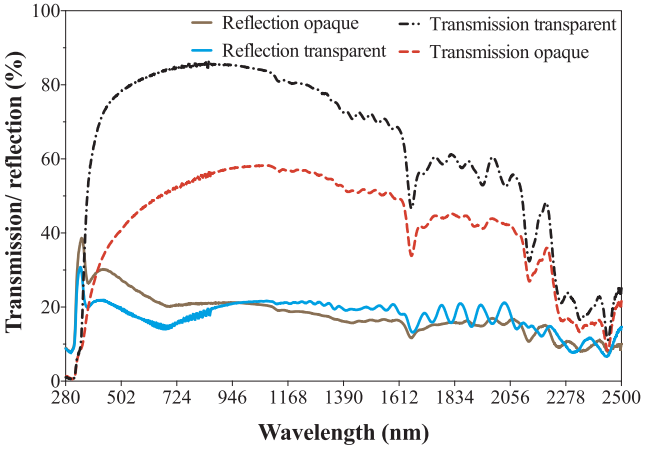

Fig. 4. Total transmission (regular + diffuse) and reflection of PDLC glazing for the transparent and translucent states.

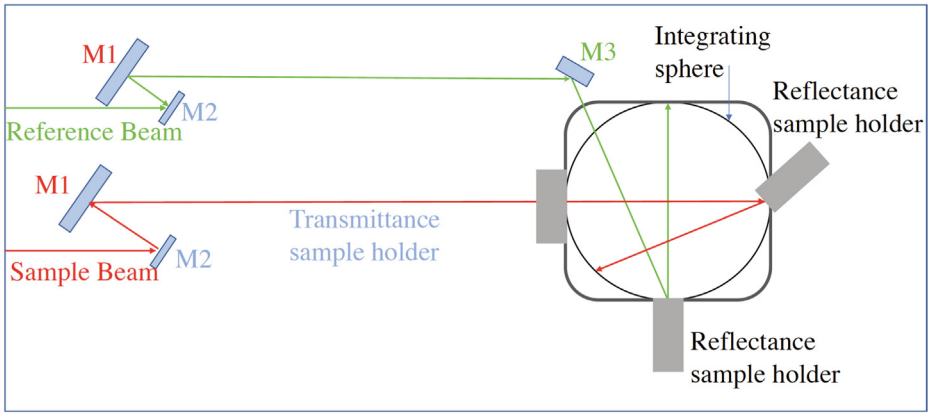

Fig. 2. Schematic diagram of Perkin Elmer® Lambda 1050 UV/VIS/NIR spectrophotometer. M1, M2, and M3 are mirrors reflecting the sample beam and reference beam.

Table 2
Measurements data of the spectrophotometer for PDLC glazing for the transparent and translucent states.

		PDLC/OFF	PDLC/ON
Solar transmittance total (300–2500)	Total	42%	62%
	Regular	12%	59%
	Diffuse	30%	4%
Solar reflectance total (300–2500)	Total	18%	17%
Visible transmittance total (380–780)	Total	44%	79%
	Regular	2%	72%
	Diffuse	42%	7%
Visible Reflectance (380–780)		24%	18%

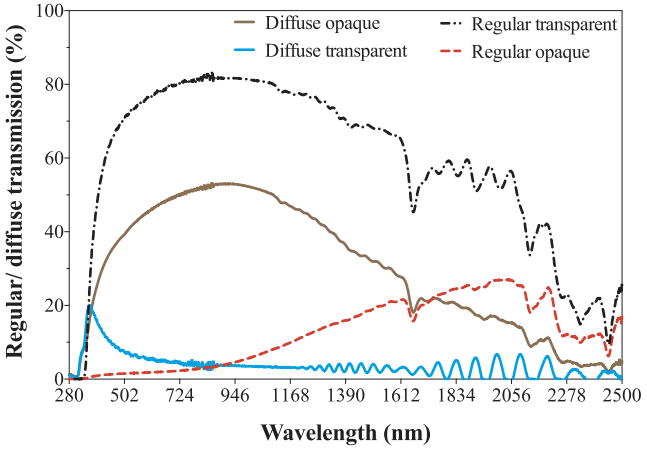

Fig. 5. Regular and diffuse transmission of PDLC glazing for the transparent state and translucent state.

Table 3
List of factor values for PDLC glazing for the transparent and translucent stats.

	PDLC/OFF	PDLC/ON
SMPF	0.69	0.39
SSPF	0.87	0.71
Selectivity index	0.7	1.16
Haze percentage	71.4%	6.4%
SHGC	0.63	0.68

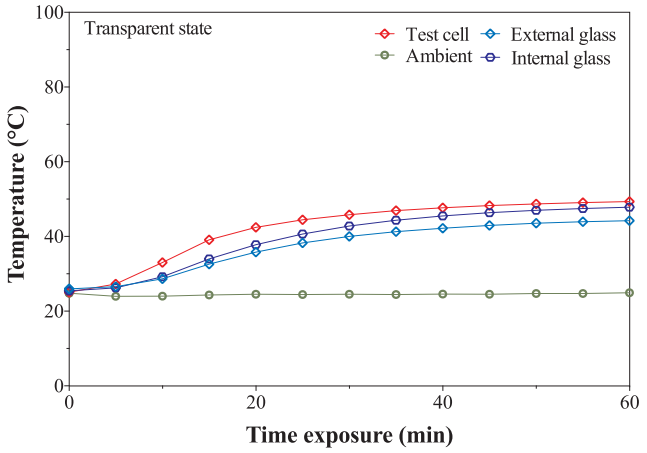

Fig. 6. Measured temperature of external and internal glazing surface, test cell and ambient environment in transparent state under 1000 W/m^2.

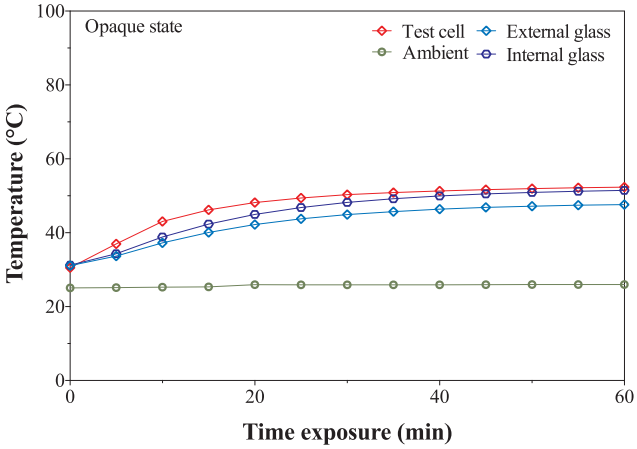

Fig. 7. Measured temperature of external and internal glazing surface, test cell and ambient environment in the translucent state under 1000 W/m^2.

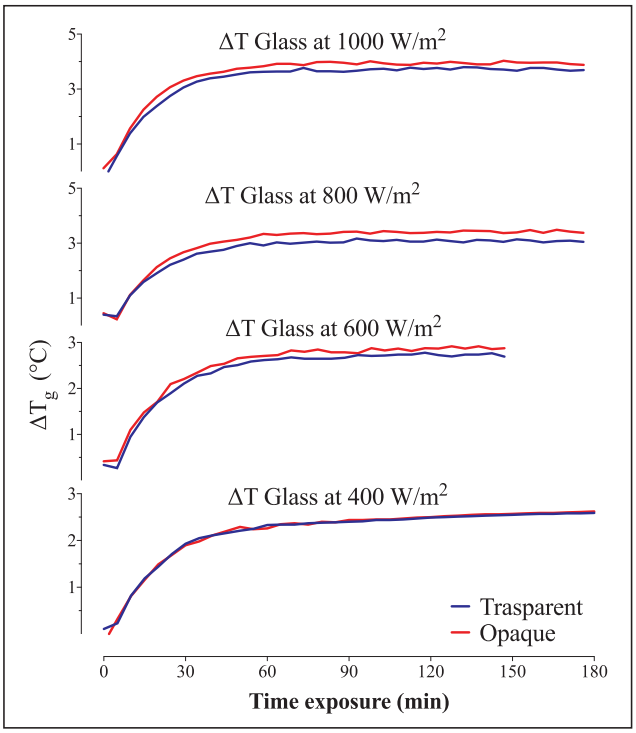

Fig. 8. The time variation of the temperature difference (ΔT_g) between the internal and external PDLC glazing surface for both the transparent (blue line) and translucent (red line) states under various radiation intensities. (For interpretation of the references to colour in this figure legend, the reader is referred to the web version of this article.)

absorption was calculated using Eq. (6), and the result was of 36% and 40% for the transparent and translucent states, respectively. The transmission measurements for PDLC glazing are presented in Table 2.

Fig. 5 reports the regular and diffuse transmissions of PDLC glazing. The regular transmission was 59% and 12% for the transparent and translucent state, respectively. Comparatively, the diffuse transmission was 4% in the transparent state and 30% in the translucent state. During the transparent state, the PDLC offers higher regular transmission and lower diffuse transmission. The higher regular transmission is a result of the alignment of the particles during the transparent (ON) state, which enables light to pass through the PDLC.

Light is scattered at a wider viewing angle in the transparent state, while the angular distribution of light can be affected by haze. From Eq. (8), haze coefficient was calculated for the transparent state and was

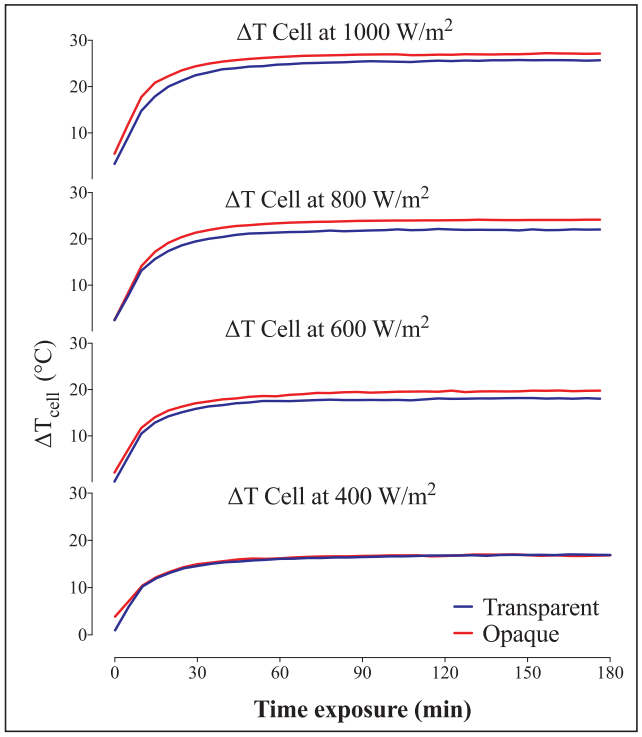

Fig. 9. The time variation of the temperature difference (ΔT_{cell}) between the test cell and the ambient temperature for both the transparent (blue line) and translucent (red line) states under various radiation intensities. (For interpretation of the references to colour in this figure legend, the reader is referred to the web version of this article.)

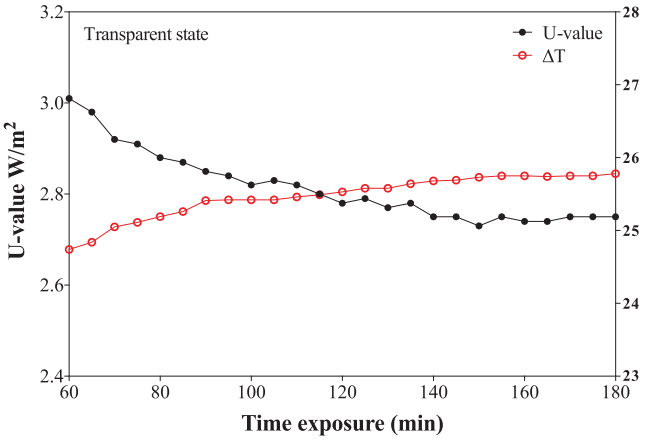

Fig. 10. *U*- value of PDLC glazing in the transparent state.

determined to be (6.4%). In contrast, the translucent state offers lower regular transmission and higher diffuse transmission. The high diffuse transmission is a result of the dispersed particles in the liquid crystal. The haze coefficient in the switch-off state was 71.4%, which is considered high value and results in the PDLC becoming translucent. Selectivity index for the investigated glazing was found to be 1.16 and 0.7 for the transparent and translucent states, respectively.

4.2. Solar material and solar skin protection factors

Solar material protection factor (SMPF) was calculated for the investigated PDLC glazing using Eq. (9) for both the transparent and translucent state, and the value was 0.39 and 0.69, respectively. Solar skin protection factor (SSPF) was found to be 0.71 for the transparent-state and 0.87 for the translucent off-state of PDLC glazing. PDLC

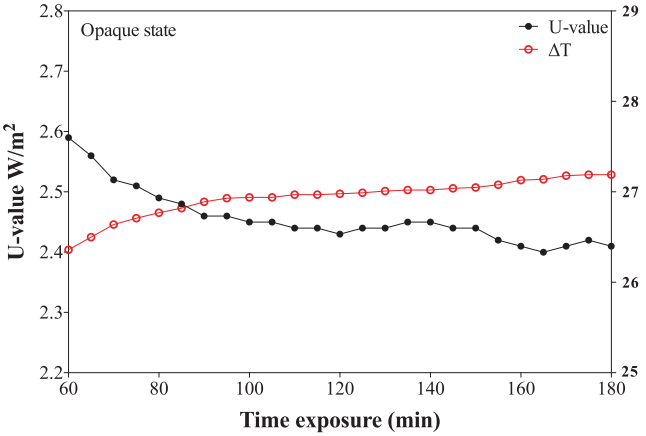

Fig. 11. *U*-value of PDLC glazing in the translucent state.

translucent state offers better protection levels for human skin and material of building interior compared to the transparent state. The SMPF and SSPF results are reported in Table 3.

4.3. PDLC glazing thermal performance

The PDLC glazing was exposed to a constant indoor solar simulator at different radiation intensities (1000, 800, 600, 400 W/m^2) for 180 min for both the transparent and translucent states. It was observed that the PDLC system behaved similarly during all various radiation intensities.

Fig. 6 illustrates the temperature variation of the system during the transparent state under the radiation of 1000 W/m^2. The test cell temperature increased from 27.3 °C to 51.22 °C following 180 min of exposure, while the ambient temperature increased from 24.00 °C to 25.54 °C. During the first 55 min, the test cell temperature increased at a rate of 2.0 °C/min, while the ambient temperature increased at 0.09 °C/min. Comparatively, it was determined that the internal glass temperature was higher than the external glass temperature, which indicates higher energy transmission; therefore, greater heat flow.

Fig. 7 presents the temperature variation of the system during the translucent state under 1000 W/m^2 radiation. In comparison, during the translucent state, the test cell temperature increased from 30.56 °C to 53.91 °C, while the ambient temperature increased from 25.07 °C to 26.78 °C for the same exposure time as the transparent state. During the first 55 min, the test cell temperature increased at a rate of 1.96 °C/min, while the ambient temperature increased at 0.084 °C/min.

Fig. 8 shows the time variation of the temperature difference (ΔT_g) between the internal and external PDLC glazing surfaces across all various radiation intensities. The temperature of the internal and external glass steadily increased for both the transparent and translucent states at a similar rate, which demonstrates that the PDLC system exhibits uniform behaviour under various radiation intensities. The average increase of temperature difference during the transparent state was 2.11 °C for all radiation intensities, while in the translucent state was 2.62 °C. It was also found that the translucent state has higher temperature differences than the transparent state. This indicates that the PDLC system exhibits higher absorption levels of radiation, rather than reflection.

Fig. 9 illustrates the time variation of the temperature difference (ΔT_{cell}) between the internal cell temperature and external ambient across all various radiation intensities. The graph highlights that the test cell has steady performance through the entire measurement. The average increase of temperature difference during the transparent state was 18.79 °C, while the translucent state was 20.12 °C under various radiation intensities. It was observed that the test cell temperature was always higher than the ambient temperature during the translucent

state, due to the absorption property of PDLC glazing, which indicates that the convection heat transfer is higher. In addition, the overall heat flow to the test cell through the PDLC glazing in the translucent state is higher compared to the transparent state. Moreover, the thermal performance of the PDLC glazing demonstrates the ability to reduce the heat loads during the cold months.

4.4. Solar heat gain coefficient (SHGC)

The solar heat gain coefficient for the PDLC glazing was found to be 0.68 and 0.63 for the transparent and translucent states, respectively. It was observed that the value of SHGC was roughly similar in both the transparent state and translucent state, due to low solar reflection and transmission in both states. In particular, high SHGC values indicate that PDLC glazing is suitable for cold climates.

4.5. Overall heat transfer (U-value)

The value of overall heat transfer was calculated when the interior and exterior glazing surfaces temperatures achieved a steady state. Fig. 10 and Fig. 11 report the PDLC glazing's *U*-value of 2.79 W/m^2 K for the transparent state and 2.44 W/m^2 K for the translucent state. The difference in the *U*-value was due to the variation of transmission of both states. The PDLC glazing *U*-value was compared to typical contemporary static transparent double glazing system. An outdoor experiment of a double glazing showed *U*-value of 2.98 W/m^2K (Ghosh et al., 2015). Thus, PDLC glazing offered 6% lower thermal transmission while the optical transmission was 32% lower than that of transparent state.

5. Conclusion

In the current study, a measurement of the optical characteristics was carried out using UV–vis–NIR (1050) spectrophotometer, and the SMPF and SSPF were calculated to evaluate a PDLC glazing system for future low energy buildings. Moreover, SHGC and *U*-value were investigated in indoor conditions. The PDLC glazing system was exposed to constant solar radiation with different radiation intensities (1000, 800, 600, 400 W/m^2) for 180 min for both the transparent (ON) and translucent (OFF) states. The results of the investigation are summarised as follow.

1. The result of the optical properties showed that the PLDC system is a good candidate for variable transparency glazing with solar modulation between 62% and 42% for the transparent and translucent states, respectively.
2. The optical evaluation showed that the investigated PDLC glazing offered low transmissions for UV (14%) and NIR (37%) in the translucent state, respectively. In addition, the system has a high degree of protecting the human skin in both states which indicate that the investigated PDLC has the potential to control the exposure to UV. The system could be significantly effective in replacing the conventional curtains as it could control the UV exposure and offer the view to the outside environment simultaneously.
3. The highest temperature for the PDLC glazing surface achieved was 52.97 °C and 49.95 °C for the translucent and transparent states, respectively, under 1000 W/m^2. In terms of the test cell, the highest temperature achieved was 53.91 °C and 51.22 °C for the translucent and transparent states, respectively. The major finding was that the PDLC glazing system demonstrated effective thermal performance in reducing heat load in a cold dominated climate with SHGC 0.68 and 0.63 for the transparent and translucent states, respectively. However, it was observed that the internal glass had a higher surface temperature, which could generate secondary heat gain resulting in thermal discomfort for the occupants.

Further investigation under real environmental conditions and computational investigation will be carried out in the future to quantify the energy-saving and energy efficiency for buildings.

Declaration of Competing Interest

The authors declare that they have no known competing financial interests or personal relationships that could have appeared to influence the work reported in this paper.

Acknowledgements

This work was conducted at the Environmental and Sustainability Institute, University of Exeter, Penryn, UK and funded by the Saudi government for higher education; the authors are grateful to the funders. This work was also supported from EPSRC_IAA (UK) fund (Grant No-EP/R511699/1) obtained by Dr Aritra Ghosh. In support of open access research, all underlying article materials (data, models) can be accessed upon request via email to the corresponding author.

References

Al Dakheel, J., Aoul, K.T., 2017. Building applications, opportunities and challenges of active shading systems: A state-of-the-art review. Energies 10. https://doi.org/10.3390/en10101672.

Baloukas, B., Arvizu, M.A., Wen, R.T., Niklasson, G.A., Granqvist, C.G., Vernhes, R., Klemberg-Sapieha, J.E., Martinu, L., 2017. Galvanostatic rejuvenation of electrochromic WO_3 thin films: ion trapping and detrapping observed by optical measurements and by time-of-flight secondary ion mass spectrometry. ACS Appl. Mater. Interfaces 9, 16995–17001. https://doi.org/10.1021/acsami.7b01260.

Barrios, D., Vergaz, R., Sanchez-Pena, J.M., Granqvist, C.G., Niklasson, G.A., 2013. Toward a quantitative model for suspended particle devices: Optical scattering and absorption coefficients. Sol. Energy Mater. Sol. Cells 111, 115–122. https://doi.org/10.1016/j.solmat.2012.12.012.

Casini, M., 2018. Active dynamic windows for buildings: A review. Renew. Energy 119, 923–934. https://doi.org/10.1016/j.renene.2017.12.049.

Casini, M., 2015. Smart windows for energy efficiency of buildings. Int. J. Civ. Struct. Eng. 2, 273–281.

Chae, Y.T., Kim, J., Park, H., Shin, B., 2014. Building energy performance evaluation of building integrated photovoltaic (BIPV) window with semi-transparent solar cells. Appl. Energy 129, 217–227. https://doi.org/10.1016/j.apenergy.2014.04.106.

Cuce, E., 2014. Development of innovative window and fabric technologies for low-carbon buildings. Univ. Nottingham.

Dussault, J.M., Gosselin, L., Galstian, T., 2012. Integration of smart windows into building design for reduction of yearly overall energy consumption and peak loads. Sol. Energy 86, 3405–3416. https://doi.org/10.1016/j.solener.2012.07.016.

European Commission, 2019. Energy performance of buildings.

Ghosh, A., Mallick, T.K., 2018a. Evaluation of optical properties and protection factors of a PDLC switchable glazing for low energy building integration. Sol. Energy Mater. Sol. Cells 176, 391–396. https://doi.org/10.1016/j.solmat.2017.10.026.

Ghosh, A., Mallick, T.K., 2018b. Evaluation of colour properties due to switching behaviour of a PDLC glazing for adaptive building integration. Renew. Energy 120, 126–133. https://doi.org/10.1016/j.renene.2017.12.094.

Ghosh, A., Norton, B., 2018. Advances in switchable and highly insulating autonomous (self-powered) glazing systems for adaptive low energy buildings. Renew. Energy 126, 1003–1031. https://doi.org/10.1016/j.renene.2018.04.038.

Ghosh, A., Norton, B., 2017. Interior colour rendering of daylight transmitted through a suspended particle device switchable glazing. Sol. Energy Mater. Sol. Cells 163, 218–223. https://doi.org/10.1016/j.solmat.2017.01.041.

Ghosh, A., Norton, B., Duffy, A., 2016a. Behaviour of a SPD switchable glazing in an outdoor test cell with heat removal under varying weather conditions. Appl. Energy 180, 695–706. https://doi.org/10.1016/j.apenergy.2016.08.029.

Ghosh, A., Norton, B., Duffy, A., 2016b. Measured thermal performance of a combined suspended particle switchable device evacuated glazing. Appl. Energy 169, 469–480. https://doi.org/10.1016/j.apenergy.2016.02.031.

Ghosh, A., Norton, B., Duffy, A., 2015. Measured overall heat transfer coefficient of a suspended particle device switchable glazing. Appl. Energy 159, 362–369. https://doi.org/10.1016/j.apenergy.2015.09.019.

Ghosh, A., Sundaram, S., Mallick, T.K., 2018. Investigation of thermal and electrical performances of a combined semi-transparent PV-vacuum glazing. Appl. Energy 228, 1591–1600. https://doi.org/10.1016/j.apenergy.2018.07.040.

Goia, F., Serra, V., 2018. Analysis of a non-calorimetric method for assessment of in-situ thermal transmittance and solar factor of glazed systems. Sol. Energy 166, 458–471. https://doi.org/10.1016/j.solener.2018.03.058.

Granqvist, C.G., Arvizu, M.A., Bayrak Pehlivan, I., Qu, H.Y., Wen, R.T., Niklasson, G.A., 2017. Electrochromic materials and devices for energy efficiency and human comfort in buildings: A critical review. Electrochim. Acta 259, 1170–1182. https://doi.org/10.1016/j.electacta.2017.11.169.

Hakemi, H.-A., Lofer, A., Peso, E., Dana, G.-F., 2018. Multiple and single layers liquid

crystal dispersion devices for common and direct glazing applications and methods thereof.
Hisham, A., Amawgani, A.H., 2019. Smart and efficient energy saving system. Smart City Symp. Prague 1–5.
Huang, J., Li, J., Xu, J., Wang, Z., Sheng, W., Li, H., Yang, Y., Song, W., 2019. Simultaneous achievement of high visible transmission and near-infrared heat shielding in flexible liquid crystal-based smart windows via electrode design. Sol. Energy 188, 857–864. https://doi.org/10.1016/j.solener.2019.06.063.
I.S.O 9050, 2003. Glass in building–Determination of light transmittance, solar direct transmittance, total solar energy transmittance, ultraviolet transmittance and related glazing factors.
Institution, B.S., 1998. Glass in Building: Determination of luminous and solar characteristics of glazing. British Standards Institution.
Jelle, B.P., 2013. Solar radiation glazing factors for window panes, glass structures and electrochromic windows in buildings - Measurement and calculation. Sol. Energy Mater. Sol. Cells 116, 291–323. https://doi.org/10.1016/j.solmat.2013.04.032.
Jelle, B.P., Gustavsen, A., Nilsen, T.N., Jacobsen, T., 2007. Solar material protection factor (SMPF) and solar skin protection factor (SSPF) for window panes and other glass structures in buildings. Sol. Energy Mater. Sol. Cells 91, 342–354. https://doi.org/10.1016/j.solmat.2006.10.017.
Jung, D., Choi, W., Park, J.Y., Kim, K.B., Lee, N., Seo, Y., Kim, H.S., Kong, N.K., 2017. Inorganic gel and liquid crystal based smart window using silica sol-gel process. Sol. Energy Mater. Sol. Cells 159, 488–495. https://doi.org/10.1016/j.solmat.2016.10.001.
Kuhn, T.E., 2017. State of the art of advanced solar control devices for buildings. Sol. Energy 154, 112–133. https://doi.org/10.1016/j.solener.2016.12.044.
Kuhn, T.E., 2014. Calorimetric determination of the solar heat gain coefficient g with steady-state laboratory measurements. Energy Build. 84, 388–402. https://doi.org/10.1016/j.enbuild.2014.08.021.
Oh, M., Lee, C., Park, J., Lee, K., Tae, S., 2019. Evaluation of Energy and Daylight Performance of Old Office Buildings in South Korea with Curtain Walls Remodeled Using Polymer Dispersed Liquid.
Park, S., Hong, J.W., 2009. Polymer dispersed liquid crystal film for variable-transparency glazing. Thin Solid Films 517, 3183–3186. https://doi.org/10.1016/j.tsf.2008.11.115.
Piccolo, A., Marino, C., Nucara, A., Pietrafesa, M., 2018. Energy performance of an electrochromic switchable glazing: Experimental and computational assessments. Energy Build. 165, 390–398. https://doi.org/10.1016/j.enbuild.2017.12.049.
Piccolo, A., Simone, F., 2015. Performance requirements for electrochromic smart window. J. Build. Eng. 3, 94–103. https://doi.org/10.1016/j.jobe.2015.07.002.
Rezaei, S.D., Shannigrahi, S., Ramakrishna, S., 2017. A review of conventional, advanced, and smart glazing technologies and materials for improving indoor environment. Sol. Energy Mater. Sol. Cells 159, 26–51. https://doi.org/10.1016/j.solmat.2016.08.026.
Salem, R., Bahadori-Jahromi, A., Mylona, A., Godfrey, P., Cook, D., 2019. Investigating the potential impact of energy-efficient measures for retrofitting existing UK hotels to reach the nearly zero energy building (nZEB) standard. Energy Effic. 1–18.
Sbar, N.L., Podbelski, L., Yang, H.M., Pease, B., 2012. Electrochromic dynamic windows for office buildings. Int. J. Sustain. Built Environ. 1, 125–139. https://doi.org/10.1016/j.ijsbe.2012.09.001.
Simmler, H., Binder, B., 2008. Experimental and numerical determination of the total solar energy transmittance of glazing with venetian blind shading. Build. Environ. 43, 197–204.
Tait, D.B., 2006. Solar heat gain coefficients for high-mass glazing blocks. ASHRAE Trans. 112.
Tavares, P., Bernardo, H., Gaspar, A., Martins, A., 2016. Control criteria of electrochromic glasses for energy savings in mediterranean buildings refurbishment. Sol. Energy 134, 236–250. https://doi.org/10.1016/j.solener.2016.04.022.
Torres, J.C., Vergaz, R., Barrios, D., Sánchez-Pena, J.M., Viñuales, A., Grande, H.J., Cabañero, G., 2014. Frequency and temperature dependence of fabrication parameters in polymer dispersed liquid crystal devices. Materials (Basel). 7, 3512–3521. https://doi.org/10.3390/ma7053512.